International Journal of Robotics and Control Systems
Vol. 4, No. 3, 2024, pp. 1109-1134
ISSN 2775-2658
http://pubs2.ascee.org/index.php/ijrcs

Novel Leak Detector Based on DWT an Experimental Study

Sabir Meftah [a,1,*], Miloud Bentoumi [a,2], Dirman Hanafi Burhanuddin [b,3], Haddi Bakhti [c,4], Chaima Chabira [a,5]

[a] LASS Laboratory of Analysis Signals and Systems, Mohamed Boudiaf University, M'sila 28000, Algeria
[b] Instrumentation and Sensing Technology (INSeT) Research Group, Faculty of Electrical and Electronic Engineering, Universiti Tun Hussein Onn Malaysia, Batu Pahat, Johor, Malaysia
[c] LGE Laboratory, Faculty of Technology, Mohamed Boudiaf University, M'sila 28000, Algeria
[1] sabir.meftah@univ-msila.dz; [2] miloud.bentoumi@univ-msila.dz; [3] dirman@uthm.edu.my;
[4] elhadi.bakhti@univ-msila.dz; [5] chaima.chabira@univ-msila.dz
* Corresponding Author

ARTICLE INFO

Article history
Received May 28, 2024
Revised June 28, 2024
Accepted July 03, 2024

Keywords
Leak;
Pressure Signal;
DWT;
DONOHO Threshold;
Detector

ABSTRACT

We always face water leakage problems in underground distribution water networks (DWNs). Existing leak detectors suffer from false alarms due to poor leak signal quality affected by external noise, often collected by acoustic or vibratory sensors. This paper introduces a novel Discrete Wavelet Transform Detector (DWTD) that leverages precise pressure signals non-influenced by environmental noise. Using a prototype of a 100m PEHD pipeline and a diameter of 40mm, Data from two pressure transmitters were collected using a dSPACE MicroLabBox unit. The main idea is to apply the Discrete Wavelet Transform (DWT) with a DONOHO threshold law to cancel noises due to water turbulence fluctuations, ensuring high-quality signals for accurate leak detection and localization. As benchmarks to assess the quality of denoising signals three parameters were calculated, Signal to Noise Ratio (SNR > 26.6763 dB), Normalized Cross-Correlation (NCC≈1), and Mean Square Error (0.20573 < MSE < 48.4761). The denoised temporal signals are obtained from the Inverse Discrete Wavelet Transform (IDWT). A Cross-correlation is employed to these signals to determine the leak's location. The experimental validation involves positioning the first and second transmitters at specific distances on both sides of the leak position. This allows for comparison between the actual leak position in advance known and calculated positions at various points and leak sizes. With only a few exceptions where the maximum error rate reached 5 meters from the actual leak position, the detector's effectiveness was proven across tests involving four different leak sizes.

1. Introduction

Both biological and industrial processes depend on water, and society suffers when this critical resource is lost. Leaks in water distribution networks (WDNs) can result in large losses of water and money. It is essential to locate and identify these leaks as soon as possible. Research conducted by the International Water Association and the World Bank [1] found that leaks cause the annual loss of about 45 million cubic meters of water. These losses have detrimental effects on the economy, especially for developing nations.

Even with the advancement of numerous leak detection techniques [2]-[12], issues like false alarms brought on by poor signal quality and outside noise interference are common with current systems. This emphasizes the requirement for a leak detection system that is more precise and dependable.

Diverse methods have been suggested by numerous studies to find water leaks. For instance, Jessica Bohorquez et al. [13] reported a method for detecting water leaks using convolutional neural networks (CNN) on pressure transient data, finding genuine pipeline leaks with a margin of error of 0.59%. Similar to, Henrik Anfinsen et al. [14] found and located leaks in branching pipeline systems and estimated the extent of the leak using parametric uncertainties and linear hyperbolic partial differential equations.

Based on these computational methods, Mohamed Waqar et al. [15] created a time inversion method to detect, classify, and calculate leak volumes. Simulations and experiments were used to confirm the method's efficiency and accuracy. Additionally, the field was advanced by I.A. Tijani et al. [16] through the development of machine learning-based leak detection algorithms. They used denoised signals to achieve high accuracy and precision in their investigation, which encompassed data collecting, signal processing, feature selection, and model creation.

Another common technique is the analysis of auditory data. To forecast leaks based on frequency domain analysis, Wenming Wang et al. [3] employed an artificial neural network model to examine the dynamic pressure distribution using sound data. Furthermore, Juma S. Tina et al. [17] created an Internet of Things (IoT) leak detection system that compares water flow measurements and finds leaks by utilizing PVC pipes, acquisition boards, and flow meter sensors.

Leak detection still heavily relies on machine learning. Machine learning algorithms were used by Tingchao Yu et al. [18] to identify leakage vibrations in actual pipeline networks while they were in operation. Additionally, the use of hydrophones for continuous water distribution network monitoring to find low-flow leaks was suggested by Konstantinos Sitaropoulos et al. [19].

To increase the precision of leak detection, sophisticated signal processing methods have been investigated. Welsh Power Spectral Density (WPSD) and Short-Time Fourier Transform (STFT) techniques were used by Miloud Bentoumi et al. [20] to discover and identify leaks in the laboratory, and their accuracy and efficiency were compared. In a water pipeline system, Haddi Bakhti et al. [21] employed a cross-correlation-based method to identify leak spots and denoise acoustic data using Empirical Mode Decomposition (EMD).

Analysis of pressure signals is one of the other creative methods. Muhammad Haziq Hakim Rosman et al. [22] developed a leak location and monitoring system by comparing pressure signals acquired in a laboratory water network to pinpoint leak locations.

Faced with the challenge of low-pressure leaks, Francis Idachaba et al. [23] proposed installing a pressure sensor in the center of the pipe, facilitating the detection of leaks otherwise undetecx by sensors located at the ends of the pipe. To support algorithm development, Mohsen Aghashahi et al. [24] published the first accessible database for recognizing and evaluating leaks.

Cross-correlation is one of the most used techniques for leak localization [25]-[37]. However, the quality of leak signals is affected by ambient noise, which is why many existing detectors, which frequently rely on vibration and acoustic sensors have false alarms [38]-[41].

Consequently, to prevent false alarms, researchers have suggested ways to filter leak signals [42]-[57]. This has significantly improved the effectiveness and success of water leak detection and localization approaches.

Many of these studies still encounter issues with signal quality and ambient noise, event thought they have greatly advanced the field of detection and localization. We suggest a unique detector that uses precise pressure signals that are unaffected by background noise, based on discrete wavelet transform (DWTD), to overcome these problems. A 100 m long high-density polyethylene (HDPE)

pipeline with pressure transmitters is part of our experimental setup. Using a professional dSPACE MicroLabBox data gathering station makes data collection easier.

The main idea is to apply the discrete wavelet transform (DWT) with a threshold determined by applying the DONOHO thresholding law. The latter is used to filter the noise of the signals acquired due to fluctuations in water turbulence in the pipe, thus guaranteeing high-quality signals and allowing precise detection and localization of leaks. Using cross-correlation gives the leak position with a minimum of error.

This work makes significant contributions to the field of water leak detection. First, we introduced an innovative leak detection system that improves signal quality through the use of DWTD. the validation of the effectiveness of our detector is done thanks to experiments carried out on previously known leaks with their positions, these tests have demonstrated its effectiveness with a minimum of errors. The current study was compared with another existing work, where we concluded the efficiency and accuracy of our proposed detector. These contributions offer a reliable solution to maintain the integrity of water distribution networks and reduce water losses in WDNs. This not only reduces water loss but also mitigates associated economic impacts, providing a valuable tool for better water management and conservation.

2. Method

The idea of our detector is inspired by work on denoising non-stationary vibration signals using the fast Fourier transform (FFT) [25]. The authors applied a threshold based on Parseval's theorem to obtain efficient filtering [25]. Subsequently, they reconstructed the denoised signal using the inverse fast Fourier transform (IFFT). Finally, they used cross-correlation to determine the delay between the two reconstructed signals. These steps are illustrated in Fig. 1 [25].

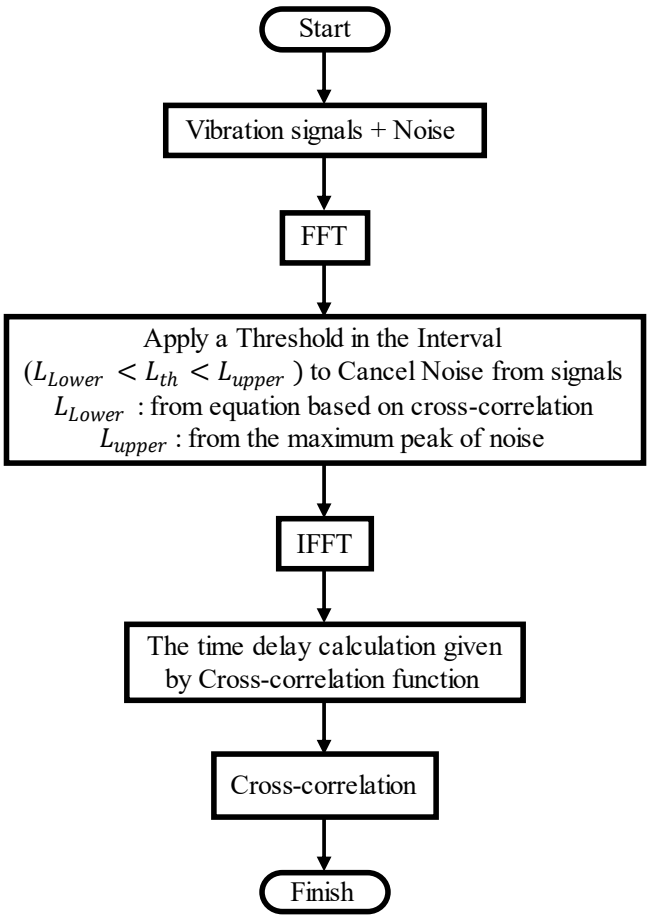

Fig. 1. Frequency noise reduction technique used for leak detection [25]

FFT analysis only gives frequency information, which means loss of temporal information, FFT cannot provide spectrum changes over time and it cannot deal with non-stationary signals [58]-[62].

In this paper, we introduce a novel Discrete Wavelet Transform Detector (DWTD) that leverages high-precision pressure transmitters (CT114-357) as illustrated in Fig. 2.

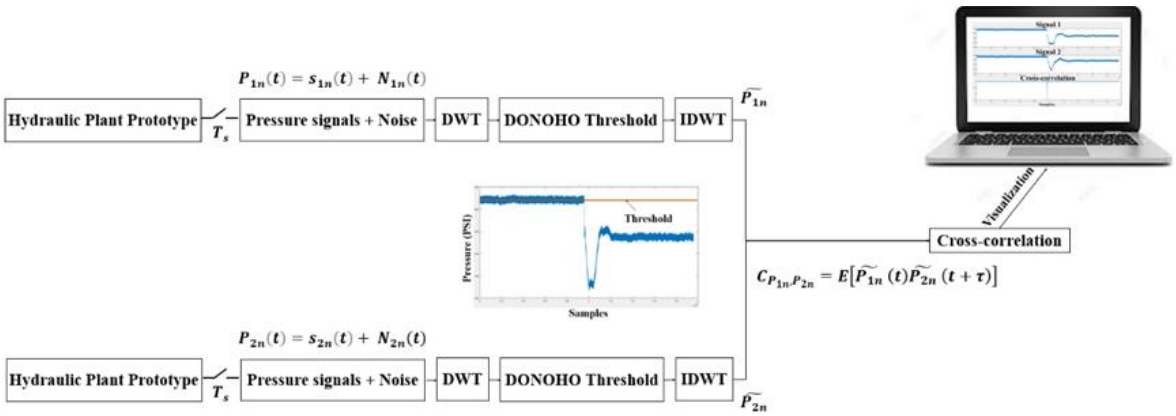

Fig. 2. The proposed detector stages

These transmitters are strategically placed on either side of the leak location: one is fixed at a predetermined distance from the leak, while the other is adjustable along the pipe up to 76m from the leak. The latter is activated by pressing a push button that controls a solenoid valve. The transmitters provide analog, linear data through a 4-20mA loop, representing the pressure information on the pipe as a current. An adapter card is used to convert the current values of the two transmitters to voltages that serve as inputs to the DSpace MicroLabBox acquisition card. The latter converts analog quantities to digital quantities with a sampling frequency of 1 kHz using two software programs (ControlDesk, and MATLAB Simulink).

A recording time of 20ms is more than enough for the acquisition of the singularity which can return to our signal. The collected pressure data is saved in the form of files with extensions.txt, and. mat. The data collected is employed offline for analysis and processing. On the latter, we will apply the DWT. A DONOHO threshold is applied to filter the acquired signals to improve the quality of the leakage signals. The quality of performance is evaluated by calculating the SNR, NCC, and MSE metrics. A reconstruction of the signals will be produced by the IDWT. A threshold equal to 10% of the smallest pressure value obtained experimentally, produced at the farthest distance will be applied to the signals obtained to confirm the presence of the leak. Once the leak is reported, its location is determined by using the correlation function. Fig. 3 illustrates the flowchart of our proposed DWTD detector.

The data collection phase contains four main sections, the hydraulic circuit, pressure transmitters, acquisition system, and the software. Fig. 4 shows the data collection process. we start by gathering the pressure signals from the hydraulic circuit using two pressure transmitters, this information will be received by the acquisition system which is connected to the computer to store, process, and visualize it using software such as (ControlDesk and MATLAB).

The dataset comprises 135 pressure measurements organized into five folders. Each folder encompasses pressure signals recorded under various conditions: absence of leaks and leaks with sizes of 4mm, 6mm, 8mm, and 12mm, labeled as S_N_L, S_L_4mm, S_L_6mm, S_L_8mm, and S_L_12mm, respectively. This data is recorded in .csv and. mat formats by the acquisition system in a duration of 20 seconds and under 1KHz frequency. Good measures mean good detection, localization, and evaluation of the leak in the water distribution pipes, for this reason, we used accurate and high-precession pressure transmitters, and we modified their position every time we wanted to record pressure information and in each of the five cases mentioned. The dSPACE MicroLabBox was additionally employed for real-time data processing, ensuring efficient operations.

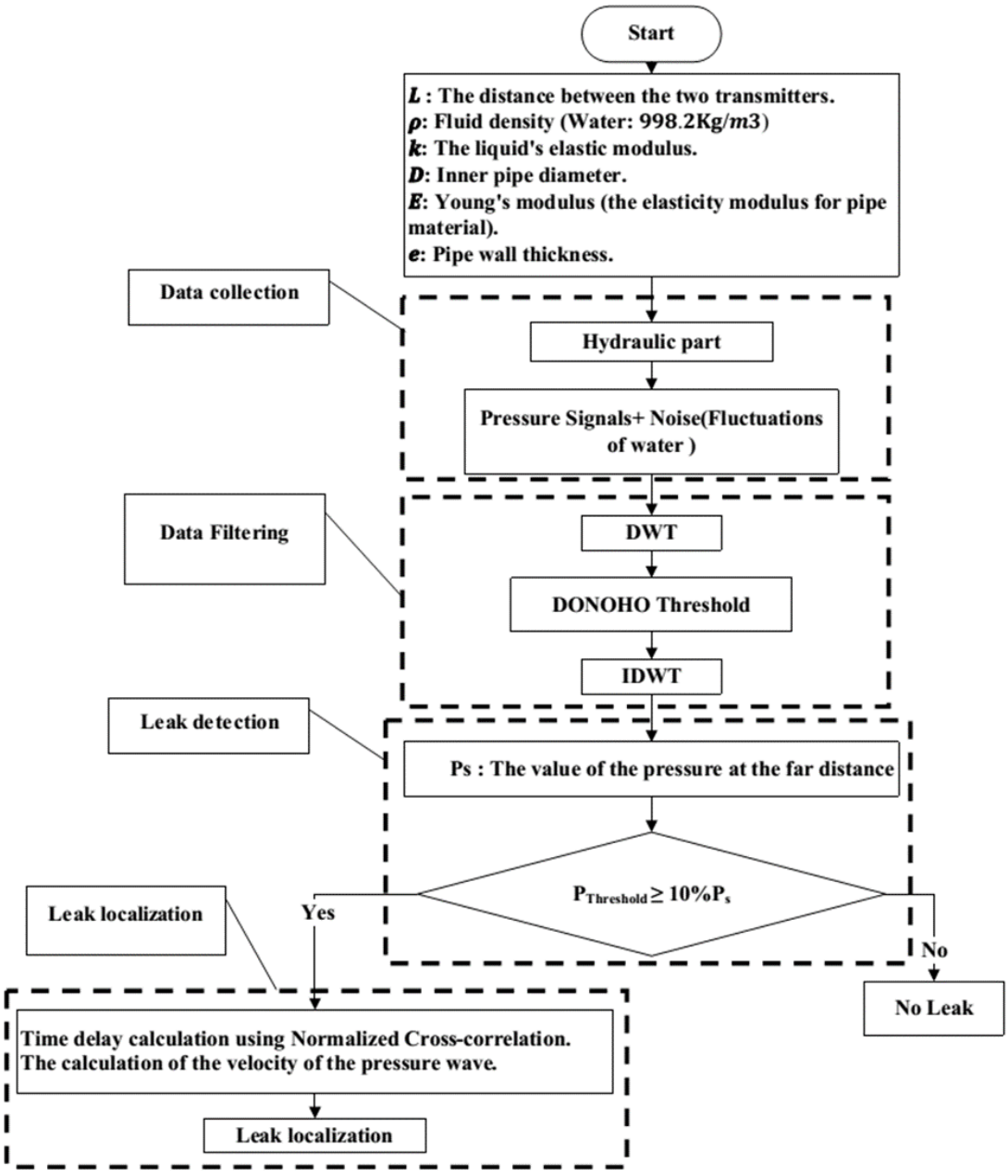

Fig. 3. Flowchart of the proposed DWTD detector

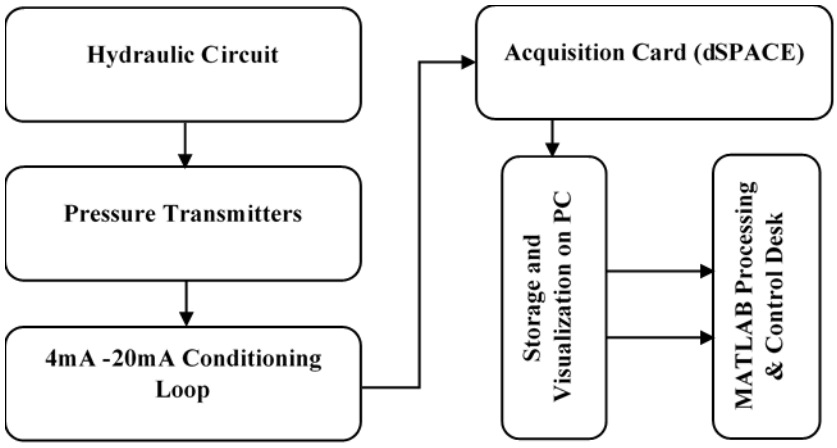

Fig. 4. Synoptic scheme of the data acquisition system

2.1. Hydraulic Circuit

In the laboratory, to implement the hydraulic circuit we used a PHDE pipe with 100m length and 0.04m diameter, and a Tank with 150L volume. A water pump was employed to transfer water from the tank to the pipeline. Additionally, various accessories were utilized to facilitate the assembly of the water pipe network. The layout of the pipe network resembles a circular configuration, as illustrated in Fig. 5.

Fig. 5. The complete hydraulic circuit

The pipe is from the K-PLAST TUBES industry in Sétif, Algeria. Where its characteristics are stated in Table 1.

Table 1. Characteristics of the pipe

Characteristics and test methods	PE 100
Dimensional characteristics	Standard: NA 7700
Melt index at 190°C-5Kg(g/10min) NA 357 /ISO 1113	0,2-0,3 g/10 min
Density NA 7603/ISO 1183	956Kg/m3
Traction characteristics NA 7701/ISO 6259	at 20°C σ = 12 MPa
Hot shrink NA 7615 /ISO 2505	≤ 3%
Hydraulic pressure resistance NA 7517/ ISO 1167	à 20°C σ = 12 MPa
Oxidation stability at 210°C NA 7705 ISO 10837	t ≥ 20 min
Dispersion of carbon black NA 7601/ISO 11420	La note < 3
Carbon black content NA 7665 /ISO 6964	< 3%
Roughness coefficient	K=0.020mm
Volatile matter content NA 7715/ISO 1269	≤ 350 mg/kg

To provide the water for the pipeline, A 150-liter tank has been used. The water went back to the tank after his circulation. Coupling, 90 Degree Elbow, Ball Valve Coupling, and PHDE Clamp Saddle, are very important accessories to implement our water network prototype.

2.2. Electrical Part

The pump is the core element of our hydraulic system, it pumps the water into the WDN. The Table 2 describes the electrical characteristics of the pump.

Table 2. Electrical characteristics of the pump

Type	PMC 3
Alimentation voltage	220v
Frequency of alimentation	50HZ
r.p.m	2850
PH~A	3.5
P2(KW)	0.6
. HP	0.8
P1(KW)	0.8
Q	100 l/min
. H	35

To achieve the objective of this article we need to collect the pressure signals of different leak diameters 4mm, 6mm, 8mm, and 12mm, to do that we used a drill with four different types of drill-bits to make holes in the pipe. The pressure transmitters catch up the signals of 20 second period under a 1Khz frequency. During the recording, we create leaks with a solenoid valve approximately 10s after the beginning of the recording process.

2.3. Pressure Transmitters

Fig. 6 illustrate the pressure transmitter used which is from Pratt & Whitney (CT114-357), and has an operating range between 1 and 100 PSIG. The pressure signals require a conditioning circuit. Due to this, these transmitters include an analog board inside of them that converts the reading's value into a value between 4 and 20 mA. Also, it has an output total error of 0.2%. The current image of the real values of pressure is modeled by Equation (1).

$$\mathrm{I(mA)} = \mathrm{a} \times \mathrm{P(PSIG)} + \mathrm{b(mA)} \tag{1}$$

Where a=0.16 and b=4mA.

The acquisition board can only read voltage signals; thus, a resistor is required to make it possible to read the value of the current flowing from the pressure transmitters.

Fig. 6. The pressure transmitter

The acquisition board can only read voltage signals; thus, a resistor is required to make it possible to read the value of the current flowing from the pressure transmitters.

2.4. Acquisition System

Using two transmitters at different points along the pipe, we were able to gather pressure data from our hydraulic network. We then read and stored the data using the dSPACE processing unit, MATLAB, and ControlDesk software, after building a Simulink circuit to connect the transmitters and the process unit, as seen in Fig. 7.

Fig. 7. Simulink circuit of the acquisition process

2.4.1. Acquisition MicroLabBox

To record large amounts of data in real-time, we employ the dSPACE MicroLabBox. The DS1104 (Master PPC) board is a data acquisition board that has 8 digital-to-analog converters (DACs) with an input voltage range of -10V to +10V, and 8 analog-to-digital converters (ADCs) with an output voltage range of -10V to +10V. It also has several interfaces, including digital input/output, incremental encoders, etc. The DS1104 also has a slave digital signal processor (DSP), the TMS320F240 DSP.

In our case, the two transmitters' pressure signals are read by analog-to-digital converter ADC1. which is a high-precision with a 16-bit resolution and a ±10 V voltage range. It has an offset error of ±5 mV and a gain error of ±0.25%, as well as a signal-to-noise ratio of >80 dB at 10 kHz. These features make it a versatile converter for measuring, controlling, and monitoring analog signals.

2.5. Discrete Wavelet Transform (DWT)

The DWT is chosen to analyze and denoise the pressure signals for its ability to provide a time-frequency representation of the signal, which is essential for non-stationary signals [63] such as pressure signals in pipes. Unlike FFT, which only includes frequency information, DWT uses a variable window to capture time and frequency information. In different fields, researchers used the discrete wavelet transform (DWT) algorithm for signal noise reduction [62]-[67]. “Wavelet transform” was first appeared in the early nineteenth century (1909) [63]. Unlike the Fourier transforms, this approach lets us utilize a changeable window based on what we require. If precision in low-frequency components is desired, a longer window is utilized; While for information in high-frequency components, a shorter window is employed. It offers a signal analysis at many resolutions. Fig. 8 illustrates multiple levels of the wavelet decomposition. Discrete wavelet transform (DWT) was applied to our non-stationary pressure signals to denoise them. The transformation Equation (2) [67].

$$DWT[a,b] = \sum_{n=0}^{N-1} x(n).\,\psi_{a,b}[n] \tag{2}$$

a, b:The scale and translation coefficient, respectively.

$x(n)$:The discrete signal.

$\psi_{a,b}[n]$:The discretized mother wavelet function.

$$\psi_{a,b}[n] = \frac{1}{\sqrt{a}}\psi\left(\frac{n-b}{a}\right) \tag{3}$$

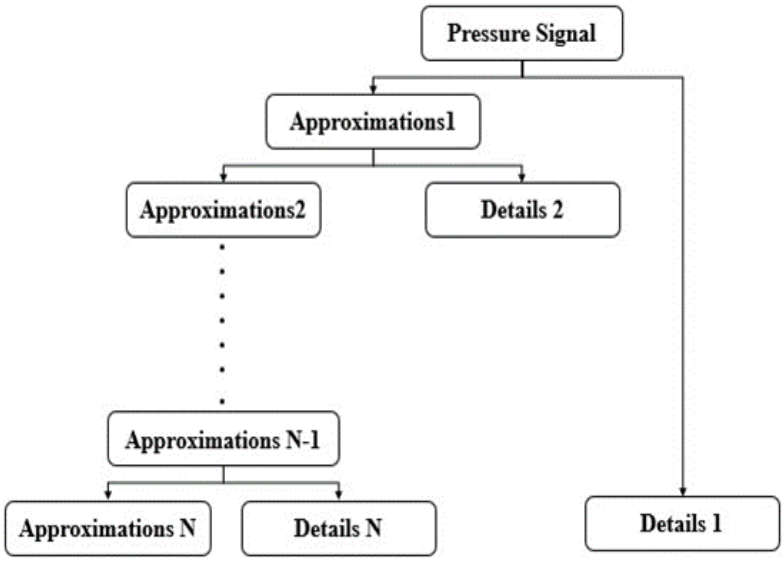

Fig. 8. Multiple-level wavelet decomposition [63]

2.5.1. Denoising with DWT

The denoising process involves applying DWT to the pressure signals, followed by soft and hard thresholding based on the DONOHO threshold to remove noise [64], [65]. The inverse DWT (IDWT) is then used to reconstruct the denoised signals. Metrics such as Signal-to-Noise Ratio (SNR), Normalized Cross-Correlation (NCC), and Mean Square Error (MSE) are calculated to evaluate the performance of the denoising process.

Soft and Hard thresholding was given by Equation (4) and Equation (5)

Soft

$$C_s = \begin{cases} 0 & , \quad |C| < T_{thr} \\ sign(C).(|C| - T_{thr}), & |C| \geq T_{thr} \end{cases} \tag{4}$$

Hard

$$C_h = \begin{cases} 0, & |C| < T_{thr} \\ C, & |C| \geq T_{thr} \end{cases} \tag{5}$$

C: The wavelet coefficients.

Donoho Thresholding

$$T_{thr} = \sigma\sqrt{2\log_2(N)} \tag{6}$$

σ: The standard deviation estimation from the median of the noisy signal.

$$\sigma = \frac{Median\ of\ wavelet\ coefficients}{0.6745} \tag{7}$$

N: The length of the noisy signal (number of samples).

T_{thr}: DONOHO coefficient threshold.

2.6. Cross-Correlation Improvement

In the event of a leak, waves propagate along the entirety of the pipe to its extremities. The interaction of physical factors, including friction, the distances between the two ends of the water transfer pipe, and the leak's location, introduces a time difference in the arrival of signals to the sensor. This time difference can be deduced by calculating the correlation between the two signal values measured simultaneously, considering the same frequency and number of samples.

In our investigation, we process pressure signals $P_{1n}[n]$ and $P_{2n}[n]$ (vectors), following the procedural steps outlined in Fig. 9. To understand their correlation, we use the cross-correlation calculation by (10). Before performing the cross-correlation calculation, a normalization of the two vectors is typically applied using a specific Equation (8) [68]. This normalization step ensures that the signals are on a comparable scale, providing a more accurate correlation measure.

$$R_{P_{1n}P_{2n}}[k] = \sum_{n=-\infty}^{\infty} P_{1n}[n]P_{2n}[n+k] \tag{8}$$

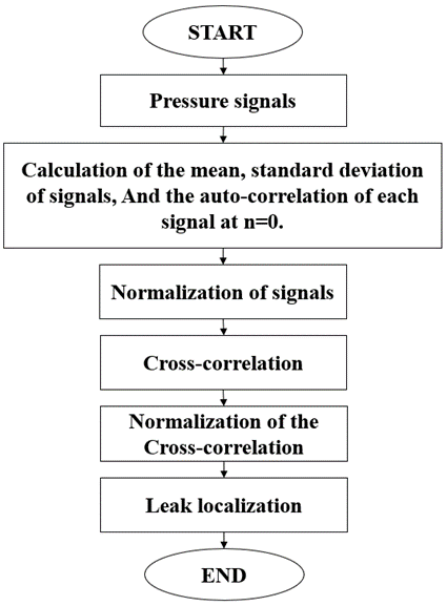

Fig. 9. Normalized Cross-correlation flowchart

To achieve cross-correlation normalization, we compute both the mean and the Traditional standard deviation of the signal. Usually calculating the mean and standard deviation enables us to account for the baseline and variability of the signals, thereby enhancing the reliability of the cross-correlation analysis [68].

$$y[n] = \frac{P[n] - \mu}{\sigma'} \tag{9}$$

$$\mu = \frac{\sum_{n=0}^{N-1} P[n]}{N} \tag{10}$$

μ :The mean of P[n].

$$\sigma' = \sqrt{\left|\frac{\sum_{n=0}^{N-1}(P[n]-\mu)^2}{N}\right|} \tag{11}$$

σ':Traditional Standard Deviation Equation.

$$\rho_{P_{1n}P_{2n}}[k] = \frac{R_{P_{1n}P_{2n}}[k]}{\sqrt{R_{P_{1n}P_{1n}}[0]R_{P_{2n}P_{2n}}[0]}} \tag{12}$$

$$\Delta t = \left(N - 1 - k_{peak}\right)/f_s \tag{13}$$

$\rho_{P_{1n}P_{2n}}[k]$:The cross-correlation between $P_{1n}[n]$ and $P_{2n}[n]$.

$R_{P_{1n}P_{1n}}[0]$, $R_{P_{2n}P_{2n}}[0]$: The autocorrelation of $P_{1n}[n]$ and $P_{2n}[n]$ at n=0.

Δt : The time difference between the two signals.

f_s : The sampling frequency.

The following Equation (14) [69] is used to compute the velocity of the pressure wave

$$v = 1\Big/\sqrt{\rho\left(\frac{1}{k}+\frac{D}{E.e}\right)} \tag{14}$$

ρ: Fluid density (Water: $998.2\text{Kg}/m^3$)

k: The liquid's elastic modulus.

D: Inner pipe diameter.

E: Young's modulus (the elasticity modulus for pipe material).

e: Pipe wall thickness.

In our case the calculated velocity v=229.785504 m/s.

After determining the Δt value and concurrently deducing the velocity v, it becomes possible to ascertain the leakage position by employing the Equation (15).

$$X = L + v\Delta t/2 \tag{15}$$

L : The distance between the two transmitters.

X : The leak position.

3. Results and Discussion

This section investigates four leak-size scenarios simulated by our prototype to emulate real-world conditions, providing an analysis of the ensuing data processing outcomes. Data collection method: At the beginning, we drilled a 4mm orifice on the pipe on which we installed a closed collar on a solenoid valve controlled by a push button simulating the leak by its opening so that we could collect the data. Then gradually in the same places the size of the orifices changes and the data is taken again. To enhance clarity in signal plotting, an amplification factor of 100 was applied. As shown in Fig. 10, for the signal without a leak from transmitter1 located 76m from the pump Fig. 10 (a), the pressure image remains stable at approximately 1.22 volts throughout the recording period. Conversely, in the case of a 4mm leak situated 2m from the leak position Fig. 10 (b). the pressure image stays stable at around 1.53 volts until the solenoid valve, which simulates the leak, is activated. About 10 seconds into the recording, a singularity is observed, causing the pressure to drop to 1.33

volts. The curve then stabilizes again at 1.45 volts. When applying the wavelet to the signal data for both without leak and leak scenarios at a chosen distance, it is evident that no significant events occur for the signal without leak Fig. 10 (a) as shown in Fig. 10 (c). However, for the signal with a leak Fig. 10, the wavelet application Fig. 10 (d) reveals spots at t=10 seconds, indicating an increase in the energy of the wavelet coefficients, particularly at t=10 seconds and scale=10, as highlighted by the color palette.

Fig. 10. The time-frequency representation of pressure signals and their wavelet scalogram

3.1. Integral State Feedback Controller

In Fig.11, two pressure signals are displayed when the first transmitter is positioned 2 meters (before the leak) and the second (after the leak) 70 meters away. The difference between the two signal amplitudes is significant, where the first amplitude is about 1,55 volts, and the second amplitude is approximately 1,28 volts. It is clear that the two signals at points (9303,154.942) and (9669,128.636), respectively, are declining. They then gradually increase after that and then stabilize at values less than before the creation of the leak. The temporal delay between the two signals is because the positions of the two transmitters are different.

3.2. Leak Size of 6mm (Noisy Signal)

In this case, transmitter one is 2 meters and transmitter two is 28 meters away from the leak position. For the first transmitter and the second transmitter, the amplitudes were respectively 1,54454 volts and 1,4423 volts before the leak occurrence. The two signals dipped after the leak was made at positions (9654,154.454) and (9794,144.23) as shown in Fig. 12, then rose once more before stabilizing.

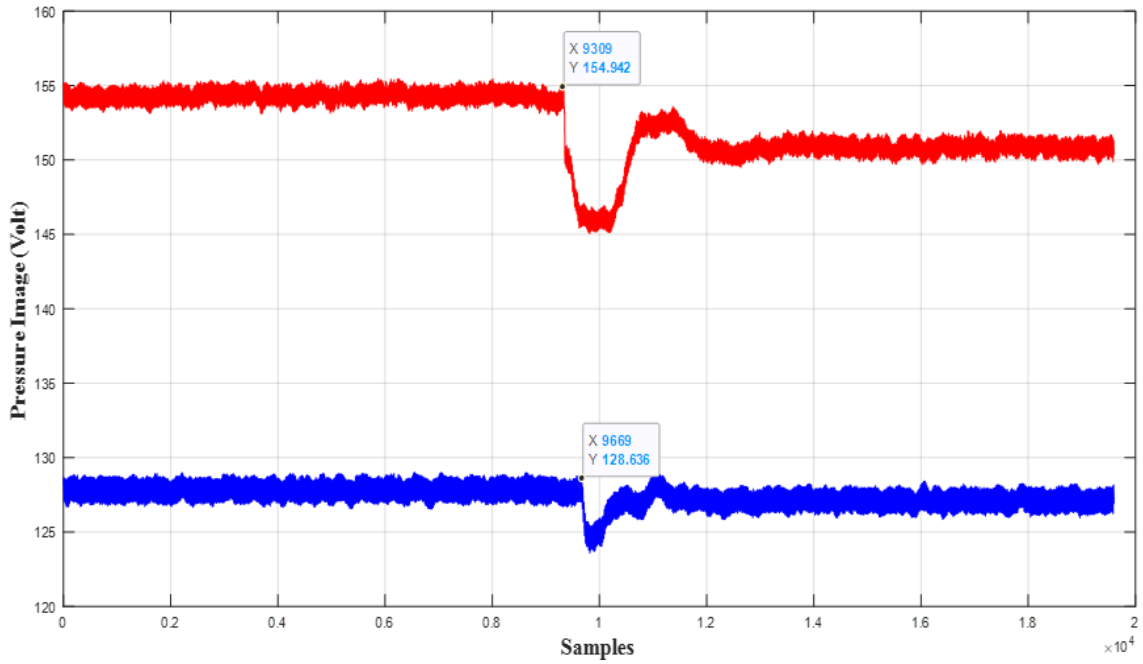

Fig. 11. Illustration of two pressure signals when a leak occurred (the first 2m and the second 70m away from the leak position)

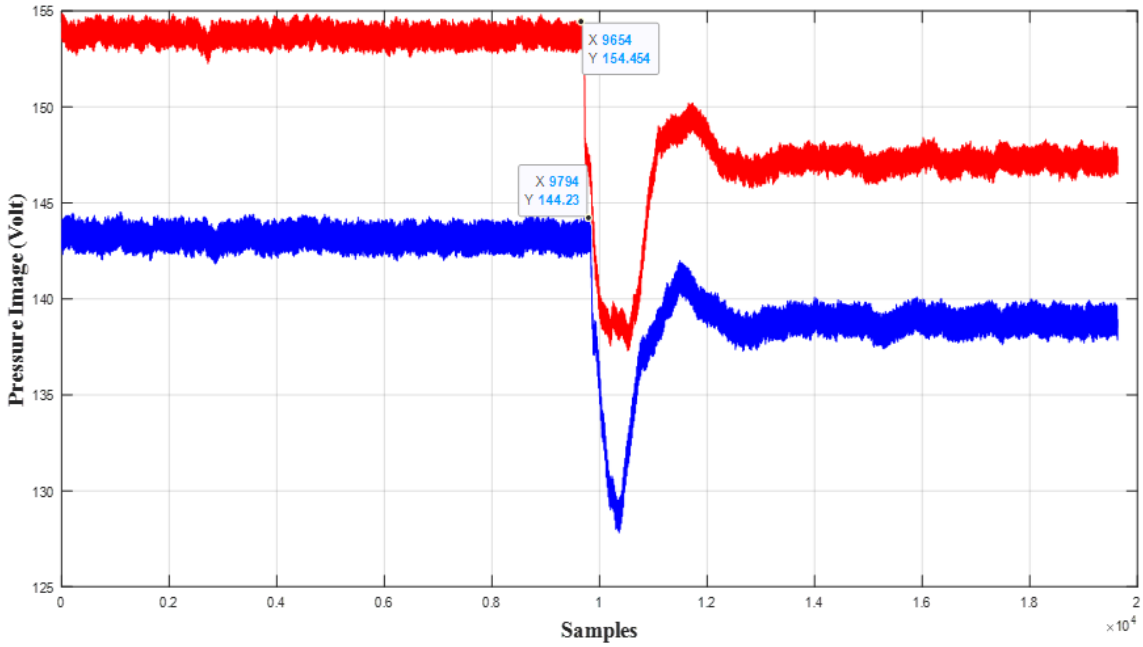

Fig. 12. Illustration of two pressure signals when a leak occurred (the first 2m and the second 28m away from the leak position)

3.3. Leak Size of 8mm (Noisy Signal)

In this scenario, transmitter one is positioned 2 meters away from the leak, while transmitter two is positioned 28 meters away. With a slight shifting and amplitude difference, both signals behaved almost identically before and after the pipe puncture as shown in Fig. 13.

3.4. Leak Size of 12mm (Noisy signal) (Noisy Signal)

In the last case where the leak with diameter of 12mm, the position of the two pressure transmitters is changed where the first one is placed at 13.5 meters and the second 76 meters away from the leak location. The signals are shown in Fig. 14.

Fig. 13. Illustration of two pressure signals when a leak occurred (the first 13.5m and the second 76m away from the leak position)

Fig. 14. Illustration of two pressure signals when a leak occurred (the first 2m and the second 28m away from the leak position)

3.5. Denoised Signals

After filtering our leakage signals, obtained in the laboratory using the DWT approach, we plotted the pressure signals at specific transmitter locations. This was done to illustrate the differences and results observed during the data collection process for leaks. Two mother wavelets (Daubechies4, Haar) at different levels were applied with the 'Soft', and 'Hard' thresholding in addition to the 'DONOHO' threshold. The following examples are given at level 4.

3.5.1. With "Daubechies4" Mother Wavelet (Db4)

Fig. 15, Fig. 16, Fig. 17, Fig. 18, Fig. 19, Fig. 20, Fig. 21, Fig. 22 illustrate the pressure signals in four cases of leakage size (4mm, 6mm, 8mm, and 12mm), where one of the cases was randomly

selected in which the first transmitter is located 2m and the second 28m before and after the real leak location. The leak is 14.5m from the entrance to the pipe network. It can be observed that the signals after filtering became smooth and no longer exhibited vibrations caused by external noise. It can be seen that as the size of the leak increases, the singularity of the signal representing the pressure decreases and varies for the wavelets Db4, Haar, and a level4 between 1.42V and 1.24V for the orifices 4 mm to 12 mm.

a. Soft Thresholding

Transsmiter 1

Fig. 15. The illustration of the denoised pressure signal captured by transmiter1 where it located 2m away from the leak in four cases: (a) At leak with size 4mm, (b) At leak with size 6mm, (c) At leak with size 8mm, (d) At leak with size 12mm. Transsmiter2

Transsmiter 2

Fig. 16. The illustration of the denoised pressure signal captured by transmiter2 which is located 28m away from the leak in four cases: (a) At leak with size 4mm, (b) At leak with size 6mm, (c) At leak with size 8mm, (d) At leak with size 12mm

b. Hard Thresholding

Transsmiter 1

Fig. 17. The illustration of the denoised pressure signal captured by transmiter1 which is located 2m away from the leak in four cases: (a) At leak with size 4mm, (b) At leak with size 6mm, (c) At leak with size 8mm, (d) At leak with size 12mm

Transsmiter 2

Fig. 18. The illustration of the denoised pressure signal captured by transmiter1 which is located 2m away from the leak in four cases: (a) At leak with size 4mm, (b) At leak with size 6mm, (c) At leak with size 8mm, (d) At leak with size 12mm

3.5.2. With "Haar" Mother Wavelet

a. Soft Thresholding

Transsmiter 1

Fig. 19. The illustration of the denoised pressure signal captured by transmiter1 where it located 2m away from the leak in four cases: (a) At leak with size 4mm, (b) At leak with size 6mm, (c) At leak with size 8mm, (d) At leak with size 12mm

Transsmiter 2

Fig. 20. The illustration of the denoised pressure signal captured by transmiter2 where it located 28m away from the leak in four cases: (a) At leak with size 4mm, (b) At leak with size 6mm, (c) At leak with size 8mm, (d) At leak with size 12mm

b. Hard Thresholding

Transsmiter 1

Fig. 21. The illustration of the denoised pressure signal captured by transmiter1 where it located 2m away from the leak in four cases: (a) At leak with size 4mm, (b) At leak with size 6mm, (c) At leak with size 8mm, (d) At leak with size 12mm

Transsmiter 2

Fig. 22. The illustration of the denoised pressure signal captured by transmiter2 where it located 28m away from the leak in four cases: (a) At leak with size 4mm, (b) At leak with size 6mm, (c) At a leak with size 8mm, (d) At leak with size 12mm

As evaluation metrics for our filtered signals, the Mean Squared Error (MSE), Normalized Cross-Correlation (NCC), and Signal-to-Noise Ratio (SNR) computed values are shown in Table 3. These characteristics shed light on how closely the filtered signals resemble the original data in terms of quality, fidelity, and similarity. A lower MSE denotes less error between the filtered and original signals, and a higher SNR denotes a stronger signal-to-noise ratio. To evaluate the efficacy of the

filtering procedure, the NCC further computes the degree of similarity between the filtered signals and the relevant references.

Table 3. Metrics of evaluation

Mother wavelet	Level	Soft threshold		Hard threshold		Soft threshold		Hard threshold		Soft threshold		Hard threshold	
		SNR				NCC				MSE			
		PT 1	PT 2	PT 1	PT 2	PT 1	PT 2	PT 1	PT 2	PT 1	PT 2	PT 1	PT 2
Db4	Level4	26.6763 dB	31.1535 dB	50.2488 dB	48.8281 dB	0.99338	0.98435	0.99338	0.98435	48.4761	15.2076	0.21295	0.25978
	Level5	29.6672 dB	34.0899 dB	50.2099 dB	48.8185 dB	0.99332	0.98432	0.99332	0.98432	24.3464	7.7344	0.21486	0.26036
	Level10	42.4097 dB	45.1296 dB	48.1564 dB	48.2039 dB	0.98311	0.97756	0.98926	0.98191	1.2947	0.60877	0.34476	0.29993
Haar	Level4	26.6769 dB	31.1568 dB	50.3985 dB	49.0283 dB	0.9936	0.98506	0.9936	0.98506	48.4694	15.1961	0.20573	0.24807
	Level5	29.6673 dB	34.0921 dB	50.2166 dB	48.8862 dB	0.99333	0.98456	0.99333	0.98456	24.3458	7.7304	0.21454	0.25633
	Level10	42.4495 dB	44.7279 dB	48.3158 dB	47.8657 dB	0.98388	0.97433	0.98965	0.98043	1.2829	0.66776	0.33233	0.32422

The analysis of Table 3 reveals a positive outcome in assessing the filtered pressure signals through the metrics SNR, NCC, and MSE. These metrics serve as crucial indicators for evaluating the efficacy of the filtration process of the signals gathered by the pressure transmitters 1 and 2 (PT1, PT2 respectively). The results indicate a notable enhancement in signal quality and a big similarity and match with the original pressure signal, substantiated by higher SNR values (SNR > 26.6763 dB), and minimized MSE (NCC≈1) values, alongside NCC (0.20573 < MSE < 48.4761) values approaching unity. Particularly noteworthy is the superior performance observed when employing a hard threshold in conjunction with a DONOHO threshold, surpassing outcomes associated with a soft threshold. This comparison underscores the significance of methodological nuances in optimizing signal filtration.

To investigate and validate the efficiency of the new proposed detector, we fill the Table 4. By a comparison of the results obtained, we can note that in general there is a great convergence between the position of the real transmitter and the calculated position, where the most estimated error was about 5 meters, and this is related to a set of factors, including the real positioning of the two transmitters. Additionally, after the creation of the leak, water erupts from the pipeline creating a turbulent jet that may indicate that the water was not at its steady state when the measurements were taken.

Table 4 presents our analysis of pressure measurements taken at various transmitter positions to calculate the change in time (ΔT) using Equations (10) and (11). This analysis forms the basis for determining the distance between the leak location and each transmitter, enabling leak localization based on collected pressure signals. For leak sizes of 4mm, 6mm, and 8mm, we positioned the first transmitter 2 meters from the actual leak, while varying the position of the second transmitter to observe different outcomes. In the case of a 12mm leak, the first sensor was placed 1.5 meters from the leak. These variations were introduced to validate the effectiveness of our proposed detector. A comparison between the actual transmitter positions and the calculated positions revealed mostly consistent results, with occasional discrepancies of up to 5 meters. This variance may be attributed to transmitter placement affecting signal quality, particularly if obstructed by structural elements or resulting in susceptibility to external noise interference.

Table 4. Experiments validation of results

Leak size	Real position		Cross-correlation value	Position calculation	
	Transmitter1	Transmitter2		Transmitter1	Transmitter2
4 MM	2m	3m	0.002s	2.2702m	2.7298m
	2m	12m	0.092s	3.5701m	17.5701m
	2m	28m	0.164s	-3.8424m	33.8424m
	2m	38m	0.12s	6.2129m	33.7871m
	2m	60m	0.216s	6.1832m	55.8168m
	2m	70m	0.304s	1.0726m	70.9274m
	2m	76m	0.336s	0.3960m	77.6040m
6MM	2m	3m	0.002s	2.2702m	2.7298m
	2m	12m	0.044s	1.9447m	12.0553m
	2m	21m	0.094s	0.7001m	22.2999m
	2m	28m	0.082s	5.5788m	24.4212m
	2m	38m	0.16s	1.6172m	38.3828m
	2m	60m	0.256s	1.5875m	60.4125m
	2m	70m	0.306s	0.8428m	71.1572m
	2m	76m	0.324s	1.7747m	76.2253m
8MM	2m	3m	0.002s	2.2702m	2.7298m
	2m	12m	0.046s	1.7149m	12.2851m
	2m	21m	0.08s	2.3086m	20.6914m
	2m	28m	0.118s	1.4427m	28.5573m
	2m	38m	0.15s	2.7661m	37.2339m
	2m	60m	0.282s	-1.3998m	63.3998m
	2m	70m	0.326s	-1.4550m	73.4550m
	2m	76m	0.328s	1.3152m	76.6848m
12MM	1.5m	9m	0.044s	0.1947	10.3053
	1.5m	14m	0.084s	-1.9010	17.4010
	1.5m	18m	0.054s	3.5458	15.9542
	1.5m	20.5m	0.058s	4.3362	17.6638
	1.5m	25m	0.064s	5.8969	20.6031
	1.5m	28.5m	0.092s	4.4299	25.5701
	1.5m	32m	0.114s	3.6522	29.8478
	1.5m	35m	0.136s	2.6246	33.8754
	1.5m	38m	0.132s	4.5842	34.9158
	1.5m	45.5m	0.148s	6.4959	40.5041
	1.5m	66m	0.234s	6.8651	60.6349
	1.5m	71.5m	0.334s	-1.8742	74.8742
	1.5m	76m	0.32s	1.9843	75.5157
	4.5m	76m	0.276s	8.5396	71.9604
	8m	76m	0.262s	11.8981	72.1019
	11m	76m	0.254s	14.3172	72.6828
	13.5m	76m	0.228s	18.5545	70.9455

Based on the content of Table 5, our comparative analysis reveals significant insights into the methodologies employed for leak detection and localization within water distribution networks. Our approach, utilizing the Discrete Wavelet Transform (DWT) and DONOHO threshold on pressure signals directly collected from transmitters, focuses on minimizing the impact of water fluctuations noise. This method ensures enhanced signal quality through precise noise reduction techniques, thereby improving the accuracy of leak detection and localization. In contrast, the existing study adopts Fast Fourier Transform (FFT) and Parseval thresholding on vibration signals, which are susceptible to external noise. Despite both studies employing cross-correlation for time delay calculation to pinpoint leak positions, our emphasis on DWT highlights its effectiveness in mitigating turbulent water fluctuations' noise, contributing to more robust leak detection systems. The comparative study underscores the importance of applied signal processing techniques in advancing the reliability and accuracy of leak detection technologies under varying environmental conditions.

Table 5. Comparison with existing work.

	Sensor Type	Signal Processing Technique	Threshold	Noise source	Leak detection	Leak Localization
Proposed DWTD Detector	Pressure Transmitters.	DWT. IDWT.	DONOHO for filtering. 10% of the value of pressure at the far distance for leak detection.	Water turbulence fluctuations.	Yes	Yes
[24]	Vibration Sensors.	FFT. IFFT.	$L_{Lower} < L_{Th} < L_{Upper}$ L_{Lower}: From equation based on Cross-correlation. L_{Upper}: From the maximum peak of noise.	Simulation of environmental noise, they consider the machinery noises as periodic signals.	Yes	Yes

4. Conclusion

Leak detection in underground distribution water networks (DWNs) remains a significant challenge, often compounded by external noise that degrades the quality of leak signals captured by acoustic or vibratory sensors. This study presents a novel Discrete Wavelet Transform Detector (DWTD) that utilizes precise pressure signals unaffected by environmental noise, thereby improving the accuracy of leak detection and localization.

The proposed detector was applied to a 100m prototype PEHD pipeline with a 40mm diameter, collecting data from two pressure transmitters via a dSPACE MicroLabBox unit. The core methodology involved applying the Discrete Wavelet Transform (DWT) with a DONOHO threshold law to filter out noise from water turbulence fluctuations, ensuring high-quality signals. The denoising process's effectiveness was evaluated using three parameters: Signal to Noise Ratio (SNR > 26.6763 dB), Normalized Cross-Correlation (NCC ≈ 1), and Mean Square Error (0.20573 < MSE < 48.4761). The denoised signals were then reconstructed using the Inverse Discrete Wavelet Transform (IDWT), and cross-correlation was used to pinpoint the leak's location.

Transmitters were placed at predetermined positions on either side of a known leak point to carry out an experimental validation. The DWTD showed promising results, with measurement errors ranging from 0.2702m to 5m, and successfully detected. These findings highlight the DWTD's potential effectiveness in practical applications, although further validation under diverse environmental and operational conditions is necessary.

Despite the DWTD's potential, several limitations need addressing. The current study was compared with another existing work, where we concluded the efficiency and accuracy of our proposed detector. However, the experimental conditions may not fully replicate real-world scenarios, and the scalability of the prototype to larger, more complex water networks remains uncertain. This study did not discuss practical considerations such as maintenance and integration with existing infrastructure. The leak position errors cotableuld be generated from the transmitter's precision, the specific configuration of the experimental setup, and the flow velocity that is calculated theoretically based on a mathematical equation.

The development of precise and reliable leak detection technologies, such as the DWTD, can greatly enhance water conservation efforts by reducing water loss and preserving vital resources. The DWTD has the potential for extensive adoption, thereby, supporting sustainability goals and combating global water scarcity. Future works should focus on the application of this detector in real-

world pipe networks to establish its general usability. It is essential to test and examine its performance in different water conditions to ensure its robustness and reliability. Furthermore, a detailed comparative analysis with existing leak detection methods will be crucial to demonstrate the DWTD's relative advantages and disadvantages in terms of accuracy, ease of implementation, and operational complexity.

Author Contribution: All authors contributed equally to the main contributor to this paper. All authors read and approved the final paper.

Funding: This research received no external funding

Conflicts of Interest: The authors declare no conflict of interest.

References

[1] Z. Zarei, E. Karami, M. Keshavarz, "Co-production of knowledge and adaptation to water scarcity in developing countries," *Journal of environmental management*, vol. 262, p. 110283, 2020, https://doi.org/10.1016/j.jenvman.2020.110283.

[2] Y. Yu, A. Safari, X. Niu, B. Drinkwater, and K. V. Horoshenkov, "Acoustic and ultrasonic techniques for defect detection and condition monitoring in water and sewerage pipes: A review," *Applied Acoustics*, vol. 183, p. 108282, 2021, https://doi.org/10.1016/j.apacoust.2021.108282.

[3] W. Wang, H. Sun, J. Guo, L. Lao, S. Wu, and J. Zhang, "Experimental study on water pipeline leak using In-Pipe acoustic signal analysis and artificial neural network prediction," *Measurement*, vol. 186, p. 110094, 2021, https://doi.org/10.1016/j.measurement.2021.110094.

[4] G. C. Giaconia *et al*., "Vibration-based water leakage detection system for public open data platforms," *The International Archives of the Photogrammetry, Remote Sensing and Spatial Information Sciences*, vol. XLVIII-4/W10-2024, pp. 71-76, 2024, https://doi.org/10.5194/isprs-archives-XLVIII-4-W10-2024-71-2024.

[5] Y. Gao, M. J. Brennan, P. F. Joseph, J. M. Muggleton, and O. Hunaidi, "On the selection of acoustic/vibration sensors for leak detection in plastic water pipes," *Journal of Sound and Vibration*, vol. 283, no. 3-5, pp. 927-941, 2005, https://doi.org/10.1016/j.jsv.2004.05.004.

[6] J. Guo *et al*., "Application of recursive VMD based on information entropy optimization in the water supply pipeline leak location," *Water Supply*, vol. 23, no. 3, pp. 1375-1389, 2023, https://doi.org/10.2166/ws.2023.071.

[7] F. Karray, A. Garcia-Ortiz, M. W. Jmal, A. M. Obeid, and M. Abid, "EARNPIPE: A Testbed for Smart Water Pipeline Monitoring Using Wireless Sensor Network," *Procedia Computer Science*, vol. 96, pp. 285-294, 2016, https://doi.org/10.1016/j.procs.2016.08.141.

[8] G. R. Anjana, K. R. S. Kumar, M. S. M. Kumar, and B. Amrutur, "A Particle Filter Based Leak Detection Technique for Water Distribution Systems," *Procedia Engineering*, vol. 119, pp. 28-34, 2015, https://doi.org/10.1016/j.proeng.2015.08.849.

[9] A. E. O. Hassan, T. A. A. Mohammed, A. DemiRkol, "Fault detection in a three-tank hydraulic system using unknown input observer and extended Kalman filter," *Journal of Engineering Research*, vol. 9, no. 4A, pp. 161-173, 2021, https://doi.org/10.36909/jer.8985.

[10] Y Y. He, S. Li and Y. Zheng, "Distributed state estimation for leak detection in water supply networks," *IEEE/CAA Journal of Automatica Sinica*, pp. 1-9, 2017, https://doi.org/10.1109/JAS.2017.7510367.

[11] N. M. Khalilabad, M. Mollazadeh, A. Akbarpour, and S. Khorashadizadeh, "Leak detection in water distribution system using non-linear Kalman filter," *International Journal of Optimization in Civil Engineering*, vol. 8, no. 2, pp. 169-180, 2018, http://ijoce.iust.ac.ir/article-1-336-en.html.

[12] S. Razvarz, R. Jafari, and A. Gegov, "Flow Modelling and Control in Pipeline Systems," *Studies in Systems, Decision and Control*, vol. 321, 2021, https://doi.org/10.1007/978-3-030-59246-2.

[13] J. Bohorquez, M. F. Lambert, B. Alexander, A. R. Simpson, and D. Abbott, "Stochastic Resonance Enhancement for Leak Detection in Pipelines Using Fluid Transients and Convolutional Neural Networks," *Journal of Water Resources Planning and Management*, vol. 148, no. 3, p. 04022001, 2022, https://doi.org/10.1061/(ASCE)WR.1943-5452.0001504.

[14] H. Anfinsen and O. M. Aamo, "Leak detection, size estimation and localization in branched pipe flows," *Automatica*, vol. 140, p. 110213, 2022, https://doi.org/10.1016/j.automatica.2022.110213.

[15] M. Waqar, M. Louati, and M. S. Ghidaoui, "Time-reversal technique for pipeline defect detection," *Water Research*, vol. 243, p. 120375, 2023, https://doi.org/10.1016/j.watres.2023.120375.

[16] I. A. Tijani, S. Abdelmageed, A. Fares, K. H. Fan, Z. Y. Hu, and T. Zayed, "Improving the leak detection efficiency in water distribution networks using noise loggers," *Science of The Total Environment*, vol. 821, p. 153530, 2022, https://doi.org/10.1016/j.scitotenv.2022.153530.

[17] J. S. Tina, B. B. Kateule, and G. W. Luwemba, "Water Leakage Detection System Using Arduino," *European Journal of Information Technologies and Computer Science*, vol. 2, no. 1, pp. 1-4, 2022, https://doi.org/10.24018/compute.2022.2.1.43.

[18] T. Yu, X. Chen, W. Yan, Z. Xu, and M. Ye, "Leak detection in water distribution systems by classifying vibration signals," *Mechanical Systems and Signal Processing*, vol. 185, p. 109810, 2023, https://doi.org/10.1016/j.ymssp.2022.109810.

[19] K. Sitaropoulos, S. Salamone, and L. Sela, "Frequency-based leak signature investigation using acoustic sensors in urban water distribution networks," *Advanced Engineering Informatics*, vol. 55, p. 101905, 2023, https://doi.org/10.1016/j.aei.2023.101905.

[20] M. Bentoumi, A. Bentoumi, and H. Bakhti, "Welsh DSP Estimate and EMD Applied to Leak Detection in a Water Distribution Pipeline," *Instrumentation Mesure Métrologie*, vol. 19, no. 1, pp. 35-41, 2020, https://doi.org/10.18280/i2m.190105.

[21] H. Bakhti, M. Bentoumi, A. Harrag, and K. El-Hadi, "Experimental Validation of Hybrid EMD-Correlation Acoustic Digital Leaks Detector in Water Distribution Network System," *Instrumentation Mesure Métrologie*, vol. 18, no. 6, pp. 535-545, 2019, https://doi.org/10.18280/i2m.180604.

[22] M. H. H. Rosman *et al*., "Real-Time Underground Plastic Pipeline Water Leakage Detection and Monitoring System," *International Journal of Robotics and Control Systems*, vol. 2, no. 2, pp. 424-434, 2022, https://doi.org/10.31763/ijrcs.v2i2.582.

[23] F. Idachaba and O. Tomomewo, "Surface pipeline leak detection using realtime sensor data analysis," *Journal of Pipeline Science and Engineering*, vol. 3, no. 2, p. 100108, 2023, https://doi.org/10.1016/j.jpse.2022.100108.

[24] M. Aghashahi, L. Sela, and M. K. Banks, "Benchmarking dataset for leak detection and localization in water distribution systems," *Data in Brief*, vol. 48, p. 109148, 2023, https://doi.org/10.1016/j.dib.2023.109148.

[25] D. Yoon, J. Park, and S. Shin, "Improvement of Cross-Correlation Technique for Leak Detection of A Buried Pipe in A Tonal Noisy Environment," *Nuclear Engineering and Technology*, vol. 44, no. 8, pp. 977-984, 2012, https://doi.org/10.5516/NET.09.2011.067.

[26] R. Ionel, S. Ionel, P. Bauer and F. Quint, "Water leakage monitoring education: Cross correlation study via spectral whitening," *IECON 2014 - 40th Annual Conference of the IEEE Industrial Electronics Society*, pp. 2465-2471, 2014, https://doi.org/10.1109/IECON.2014.7048851.

[27] M. Kothandaraman, Z. Law, E. M. A. Gnanamuthu and C. H. Pua, "An Adaptive ICA-Based Cross-Correlation Techniques for Water Pipeline Leakage Localization Utilizing Acousto-Optic Sensors," *IEEE Sensors Journal*, vol. 20, no. 17, pp. 10021-10031, 2020, https://doi.org/10.1109/JSEN.2020.2991639.

[28] S. B. Beck, M. D. Curren, N. D. Sims, and R. Stanway, "Pipeline Network Features and Leak Detection by Cross-Correlation Analysis of Reflected Waves," *Journal of Hydraulic Engineering*, vol. 131, no. 8, pp. 715-723, 2005, https://doi.org/10.1061/(ASCE)0733-9429(2005)131:8(715).

[29] Y. Gao, M. J. Brennan, and P. F. Joseph, "On the effects of reflections on time delay estimation for leak detection in buried plastic water pipes," *Journal of Sound and Vibration*, vol. 325, no. 3, pp. 649-663, 2009, https://doi.org/10.1016/j.jsv.2009.03.037.

[30] M. F. Ghazali, S. B. M. Beck, J. D. Shucksmith, J. B. Boxall, and W. J. Staszewski, "Comparative study of instantaneous frequency based methods for leak detection in pipeline networks," *Mechanical Systems and Signal Processing*, vol. 29, pp. 187-200, 2012, https://doi.org/10.1016/j.ymssp.2011.10.011.

[31] F. C. L. Almeida, M. J. Brennan, P. F. Joseph, Y. Gao, and A. T. Paschoalini, "The effects of resonances on time delay estimation for water leak detection in plastic pipes," *Journal of Sound and Vibration*, vol. 420, pp. 315-329, 2018, https://doi.org/10.1016/j.jsv.2017.06.025.

[32] M. J. Brennan, Y. Gao, P. C. Ayala, F. C. L. Almeida, P. F. Joseph, and A. T. Paschoalini, "Amplitude distortion of measured leak noise signals caused by instrumentation: Effects on leak detection in water pipes using the cross-correlation method," *Journal of Sound and Vibration*, vol. 461, p. 114905, 2019, https://doi.org/10.1016/j.jsv.2019.114905.

[33] Y. Gao, M. J. Brennan, Y. Liu, F. C. L. Almeida, and P. F. Joseph, "Improving the shape of the cross-correlation function for leak detection in a plastic water distribution pipe using acoustic signals," *Applied Acoustics*, vol. 127, pp. 24-33, 2017, https://doi.org/10.1016/j.apacoust.2017.05.033.

[34] H. Liang, Y. Gao, H. Li, S. Huang, M. Chen, and B. Wang, "Pipeline Leakage Detection Based on Secondary Phase Transform Cross-Correlation," *Sensors*, vol. 23, no. 3, p. 1572, 2023, https://doi.org/10.3390/s23031572.

[35] S. B. Sharkova and V. A. Faerman, "Wavelet transform-based cross-correlation in the time-delay estimation applications," *Journal of Physics: Conference Series*, vol. 2142, no. 1, p. 012019, 2021, https://doi.org/10.1088/1742-6596/2142/1/012019.

[36] M. J. Brennan, P. F. Joseph, J. M. Muggleton, and Y. Gao, M, "Some recent research results on the use of acoustic methods to detect water leaks in buried plastic water pipes," *Institute of Sound and Vibration Research, University of Southampton*, pp. 1-7, 2005, https://www.southampton.ac.uk/assets/imported/transforms/content-block.

[37] S. El-Zahab, T. Zayed, "Leak detection in water distribution networks: an introductory overview," *Smart Water*, vol. 4, no. 1, p. 5, https://doi.org/10.1186/s40713-019-0017-x.

[38] Y. Wu and S. Liu, "A review of data-driven approaches for burst detection in water distribution systems," *Urban Water Journal*, vol. 14, no. 9, pp. 972-983, 2017, https://doi.org/10.1080/1573062X.2017.1279191.

[39] A. Blázquez-García, A. Conde, U. Mori, and J. A. Lozano, "Water leak detection using self-supervised time series classification," *Information Sciences*, vol. 574, pp. 528-541, 2021, https://doi.org/10.1016/j.ins.2021.06.015.

[40] M. Romano, Z. Kapelan, and D. A. Savić, "Real-Time Leak Detection in Water Distribution Systems," *Water Distribution Systems Analysis 2010*, pp. 1074-1082, 2011, https://doi.org/10.1061/41203(425)97.

[41] N. A. Mohd Yussof and H. W. Ho, "Review of Water Leak Detection Methods in Smart Building Applications," *Buildings*, vol. 12, no. 10, p. 1535, 2022, https://doi.org/10.3390/buildings12101535.

[42] O. Scussel, M. J. Brennan, F. C. L. Almeida, J. M. Muggleton, E. Rustighi, and P. F. Joseph, "Estimating the spectrum of leak noise in buried plastic water distribution pipes using acoustic or vibration measurements remote from the leak," *Mechanical Systems and Signal Processing*, vol. 147, p. 107059, 2021, https://doi.org/10.1016/j.ymssp.2020.107059.

[43] M. D. Kafle, S. Fong, and S. Narasimhan, "Active acoustic leak detection and localization in a plastic pipe using time delay estimation," *Applied Acoustics*, vol. 187, p. 108482, 2022, https://doi.org/10.1016/j.apacoust.2021.108482.

[44] P. Zhang *et al*., "Ground vibration analysis of leak signals from buried liquid-filled pipes: An experimental investigation," *Applied Acoustics*, vol. 200, p. 109054, 2022, https://doi.org/10.1016/j.apacoust.2022.109054.

[45] O. Scussel *et al*., "Analysis of phase data from ground vibration measurements above a leaking plastic water pipe," *Journal of Sound and Vibration*, vol. 564, p. 117873, 2023, https://doi.org/10.1016/j.jsv.2023.117873.

[46] W. Wang and Y. Gao, "Pipeline leak detection method based on acoustic-pressure information fusion," *Measurement*, vol. 212, p. 112691, 2023, https://doi.org/10.1016/j.measurement.2023.112691.

[47] J. Jiao, J. Zhang, Y. Ren, G. Li, B. Wu, and C. He, "Sparse representation of acoustic emission signals and its application in pipeline leak location," *Measurement*, vol. 216, p. 112899, 2023, https://doi.org/10.1016/j.measurement.2023.112899.

[48] D. A. Otchere, A. H. Latiff, and B. N. Tackie-Otoo, "Distributed acoustic sensing in subsurface applications – Review and potential integration with artificial intelligence for an intelligent CO2 storage monitoring system," *Geoenergy Science and Engineering*, vol. 237, p. 212818, 2024, https://doi.org/10.1016/j.geoen.2024.212818.

[49] L. Yao, Y. Zhang, T. He, and H. Luo, "Natural gas pipeline leak detection based on acoustic signal analysis and feature reconstruction," *Applied Energy*, vol. 352, p. 121975, 2023, https://doi.org/10.1016/j.apenergy.2023.121975.

[50] L. Bykerk and J. Valls Miro, "Vibro-Acoustic Distributed Sensing for Large-Scale Data-Driven Leak Detection on Urban Distribution Mains," *Sensors*, vol. 22, no. 18, p. 6897, 2022, https://doi.org/10.3390/s22186897.

[51] Z. Ahmad, T. Nguyen, A. Rai, and J. Kim, "Industrial fluid pipeline leak detection and localization based on a multiscale Mann-Whitney test and acoustic emission event tracking," *Mechanical Systems and Signal Processing*, vol. 189, p. 110067, 2023, https://doi.org/10.1016/j.ymssp.2022.110067.

[52] H. Fan, S. Tariq, and T. Zayed, "Acoustic leak detection approaches for water pipelines," *Automation in Construction*, vol. 138, p. 104226, 2022, https://doi.org/10.1016/j.autcon.2022.104226.

[53] Y. Wu *et al*., "Hybrid method for enhancing acoustic leak detection in water distribution systems: Integration of handcrafted features and deep learning approaches," *Process Safety and Environmental Protection*, vol. 177, pp. 1366-1376, 2023, https://doi.org/10.1016/j.psep.2023.08.011.

[54] K. Wang, Y. Hu, M. Qin, G. Liu, Y. Li, and G. Wang, "A leakage particle–wall impingement based vibro-acoustic characterization of the leaked sand–gas pipe flow," *Particuology*, vol. 55, pp. 84-93, 2021, https://doi.org/10.1016/j.partic.2020.07.005.

[55] M. Boujelben, Z. Benmessaoud, M. Abid, and M. Elleuchi, "An efficient system for water leak detection and localization based on IoT and lightweight deep learning," *Internet of Things*, vol. 24, p. 100995, 2023, https://doi.org/10.1016/j.iot.2023.100995.

[56] R. Vanijjirattikhan *et al*., "AI-based acoustic leak detection in water distribution systems," *Results in Engineering*, vol. 15, p. 100557, 2022, https://doi.org/10.1016/j.rineng.2022.100557.

[57] R. Müller *et al*., "Acoustic Leak Detection in Water Networks," *Proceedings of the 13th International Conference on Agents and Artificial Intelligence - Volume 2*, pp. 306-313, 2021, https://doi.org/10.5220/0010295403060313.

[58] A. Lay-Ekuakille, G. Vendramin, A. Trotta, and P. Vanderbemden, "STFT-based spectral analysis of urban waterworks leakage detection," *International Measurement Confederation*, pp. 2172-2176, 2009, https://www.imeko.org/publications/wc-2009/IMEKO-WC-2009-TC19-147.pdf.

[59] A. Lay-Ekuakille, A. Trotta and G. Vendramin, "FFT- based spectral response for smaller pipeline leak detection," *2009 IEEE Instrumentation and Measurement Technology Conference*, pp. 328-331, 2009, https://doi.org/10.1109/IMTC.2009.5168469.

[60] A. Lay-Ekuakille, A. Trotta, G. Vendramin and P. Vanderbemdem, "FFT- based algorithm improvements for detecting leakage in pipelines," *2009 6th International Multi-Conference on Systems, Signals and Devices*, pp. 1-4, 2009, https://doi.org/10.1109/SSD.2009.4956691.

[61] A. Lay-Ekuakille, G. Vendramin and A. Trotta, "Robust Spectral Leak Detection of Complex Pipelines Using Filter Diagonalization Method," *IEEE Sensors Journal*, vol. 9, no. 11, pp. 1605-1614, 2009, https://doi.org/10.1109/JSEN.2009.2027410.

[62] P. Karthikeyan, M. Murugappan, and S. Yaacob, "ECG Signal Denoising Using Wavelet Thresholding Techniques in Human Stress Assessment," *International Journal of Electrical Engineering and Informatics*, vol. 4, no. 2, pp. 306-319, 2012, https://doi.org/10.15676/ijeei.2012.4.2.9.

[63] C. K. Chui, "An Introduction to Wavelets," *Academic Press*, vol. 60, no. 202, p. 854, 1993, https://doi.org/10.2307/2153134.

[64] R. Aggarwal, J. Karan Singh, V. Kumar Gupta, S. Rathore, M. Tiwari, and A. Khare, "Noise Reduction of Speech Signal using Wavelet Transform with Modified Universal Threshold," *International Journal of Computer Applications*, vol. 20, no. 5, pp. 14-19, 2011, https://doi.org/10.5120/2431-3269.

[65] S. Lahmiri, "Comparative study of ECG signal denoising by wavelet thresholding in empirical and variational mode decomposition domains," *Healthcare Technology Letters*, vol. 1, no. 3, pp. 104-109, 2014, https://doi.org/10.1049/htl.2014.0073.

[66] Ç. P. Dautov and M. S. Özerdem, "Wavelet transform and signal denoising using Wavelet method," *2018 26th Signal Processing and Communications Applications Conference (SIU)*, pp. 1-4, 2018, https://doi.org/10.1109/SIU.2018.8404418.

[67] C. Polat and M. S. Özerdem, "Introduction to Wavelets and their applications in signal denoising," *Bitlis Eren University Journal of Science and Technology*, vol. 8, no. 1, pp. 1-10, 2018, https://doi.org/10.17678/beuscitech.349020.

[68] J. Li, S. Chen, Y. Zhang, S. Jin and L. Wang, "Cross-Correlation Method for Online Pipeline Leakage Monitoring System," *2009 2nd International Congress on Image and Signal Processing*, pp. 1-4, 2009, https://doi.org/10.1109/CISP.2009.5302839.

[69] P. Ostapkowicz, "Leakage detection from liquid transmission pipelines using improved pressure wave technique," *Eksploatacja i Niezawodność*, vol. 16, no. 1, pp. 9-16, 2014, http://www.ein.org.pl/sites/default/files/2014-01-02.pdf.